

DMD #9894

## Disposition of [ $^{14}\text{C}$ ] Ruboxistaurin in Humans

Jennifer L. Burkey, Kristina M. Campanale, Robert Barbuch, Douglas O'Bannon, James  
Rash, Charles Benson and David Small

Lilly Research Laboratories, A Division of Eli Lilly and Company, Lilly Corporate  
Center, and Lilly Laboratory for Clinical Research, Indiana University Hospital and  
Outpatient Center, Indianapolis, IN (JLB, KMC, RB, DO, JR, CB, DS)

DMD #9894

Running Title: Human [<sup>14</sup>C]ruboxistaurin

Requests for reprints should be sent to:

Dr. Jennifer Burkey

Lilly Research Laboratories

A Division of Eli Lilly and Company

Lilly Corporate Center

Indianapolis, IN 46285 USA

Phone (317) 433 – 5860

Fax (317) 433 – 6432

[Burkey\\_jennifer\\_1@lilly.com](mailto:Burkey_jennifer_1@lilly.com)

Lilly Research Laboratories

A Division of Eli Lilly and Company

Lilly Corporate Center

Lilly Laboratory for Clinical Research

Indiana University Hospital and Outpatient Center

Text pages: 17

Tables: 5

Figures: 7

References: 25

Words in Abstract: 226

Words in Introduction: 454

Words in Discussion: 768

DMD #9894

## **Abstract:**

Ruboxistaurin is a potent and specific inhibitor of the  $\beta$  isoforms of Protein Kinase C (PKC) which is being developed for the treatment of diabetic microvascular complications. The disposition of [ $^{14}\text{C}$ ]ruboxistaurin was determined in six healthy male subjects who received a single oral dose of 64 mg [ $^{14}\text{C}$ ]ruboxistaurin in solution. There were no clinically significant adverse events during the study. Whole blood, urine, and feces were collected at frequent intervals after dosing. Metabolites were profiled by high performance liquid chromatography (HPLC) with radiometric detection. The total mean recovery of the radioactive dose was approximately 87%, with the majority of the radioactivity ( $82.6 \pm 1.1\%$ ) recovered in the feces. Urine was a minor pathway of elimination ( $4.1 \pm 0.3\%$ ). The major route of ruboxistaurin metabolism was to the N-desmethyl ruboxistaurin metabolite (LY338522), which has been shown to be active and equipotent to ruboxistaurin in the inhibition of PKC $\beta$ . In addition, multiple hydroxylated metabolites were identified by LC/MS in all matrices. Pharmacokinetics were conducted for both ruboxistaurin and LY338522 (N-desmethyl ruboxistaurin, 1). These moieties together accounted for approximately 52% of the radiocarbon measured in the plasma. The excreted radioactivity was profiled using radiochromatography and approximately 31% was structurally characterized as ruboxistaurin or N-desmethyl ruboxistaurin. These data demonstrate that ruboxistaurin is metabolized primarily to N-desmethyl ruboxistaurin (1) and multiple other oxidation products, and is excreted primarily in the feces.

## Introduction:

Protein kinase C (PKC) is a group of isozymes important in signal transduction and intracellular signaling through diacylglycerol. In diabetes, hyperglycemia-induced generation of diacylglycerol selectively activates the  $\beta_2$  isoform of PKC, and increases in diacylglycerol and PKC activity have been measured in the retina, kidneys, aorta, and heart, all organs that are known to develop diabetic complications associated with the vasculature (Craven and DeRubertis 1989; Ayo et al. 1991; Inoguchi et al. 1992; Shiba et al. 1993, Craven et al. 1990, Williams and Schrier 1992; Williams and Schrier 1993; Kikkawa et al. 1994; DeRubertis and Craven 1994). The selective inhibition of PKC $\beta$  has been shown to inhibit diabetes-induced abnormalities in retinal blood flow and intraocular neovascularization caused by retinal ischemia in animals (Danis et al. 1998, Kowluru et al. 1998). These data suggest that hyperglycemia and the resulting activation of PKC $\beta$  may contribute to the development of diabetic complications. Further, a selective PKC $\beta$  inhibitor may be of benefit in the treatment of diabetic complications by blocking this mechanism.

Ruboxistaurin (Figure 1), (*S*)-13-[(dimethylamino)methyl]-10,11,14,15-tetrahydro-4,9:16,21-dimetheno-1*H*,13*H*-dibenzo[*E,K*]pyrrolo-[3,4-*H*][1,4,13]oxadiazacyclohexadecene-1,3(2*H*)-dione, is a potent and specific inhibitor of PKC $\beta$  (Jirousek et al. 1996). Previous studies have shown that ruboxistaurin (LY333531) was effective in reversing vascular abnormalities induced in diabetic animals (Ishii et al. 1996) and that diabetes-induced elevations in PKC activity in the retina and kidneys of diabetic animals were normalized (Kowluru et al. 1996). Clinical studies have shown, following administration of ruboxistaurin, an amelioration of abnormal retinal hemodynamics in

DMD #9894

patients with diabetes (Aiello et al. 1999), prevention of the reduction in endothelium-dependent vasodilatation induced by acute hyperglycemia (Beckman, et al. 2002), and have demonstrated promising results in patients with diabetic retinopathy (PKC-DRS Study Group 2005, Aiello et al. 2005) and diabetic nephropathy (Tuttle et al. 2005). Thus it is thought that ruboxistaurin may be useful in slowing the progression of diabetic complications.

In vitro metabolism of ruboxistaurin in dog, human and rat liver microsomes and fresh liver slices, as well as in vivo metabolism studies in dog, rat, and mouse, have resulted in the identification of multiple metabolites (Barbuch et al. 2006). LY338522 (N-desmethyl ruboxistaurin) was identified in preliminary metabolism studies as a major metabolite of ruboxistaurin, and was found to be equally potent to the parent in the inhibition of PKC $\beta$  (Jirousek et al. 1996). N-desmethyl ruboxistaurin has also been detected in the plasma of animals and humans following oral administration of ruboxistaurin and, therefore, has been considered when estimating the overall exposure to active molecule in clinical studies.

The study described here was designed to assess the disposition of ruboxistaurin after a single oral dose of 64 mg of [ $^{14}\text{C}$ ] ruboxistaurin containing approximately 100  $\mu\text{Ci}$  of radioactivity administered to healthy male subjects, and to examine the metabolites produced in humans.

DMD #9894

## Materials and Methods:

**Chemicals:** Ruboxistaurin, [<sup>14</sup>C]ruboxistaurin (Figure 1), and standards of metabolites 1, 2, 3, 5, and 28 were synthesized or prepared at Eli Lilly and Company, Indianapolis, IN. The structures of these metabolites are described in Table 4 of this manuscript. All other materials were of HPLC or analytical grade. [<sup>14</sup>C]ruboxistaurin was assayed and found to be 99.8% pure with a specific activity of 97.3 μCi/mg.

**Dose Formulation:** Doses were prepared as a dry blend of both radiolabeled and unlabeled ruboxistaurin. Just prior to administration, the powder was dissolved in extremely dilute phosphoric acid (3.3% phosphoric acid) to provide approximately 64 mg ruboxistaurin (free base) with approximately 100 μCi of radioactivity in an oral solution. Assayed samples were found to contain 66 mg ruboxistaurin and 102 μCi of radioactivity.

**Study Design.** Six healthy male volunteers between 19 and 49 years old participated in this single dose open label study. Informed consent was obtained according to the ethical principles stated in the latest version of the Declaration of Helsinki, the applicable guidelines for good clinical practice, and the applicable laws and regulations of the United States, whichever provided the greatest protection of the individual. The drug was administered as a single oral dose of 64 mg [<sup>14</sup>C]ruboxistaurin in solution, given in 200 mL diluent followed by a further 200 mL water or diluent used to rinse the container. The dose was administered within 15 minutes following consumption of a high calorie meal to maximize bioavailability.

DMD #9894

Blood, urine, and feces were collected before and after study drug administration. Heparinized blood (10 mL) was collected at approximately time 0 (predose), 0.5, 1, 2, 3, 4, 5, 6, 8, 12, 24, 36, 48, 72, and 96 hours after dosing for determination of radioactivity in blood and plasma and for determination of plasma ruboxistaurin and N-desmethyl ruboxistaurin concentrations. Additional blood samples were collected for determination of potential metabolites in plasma. Plasma was obtained from whole blood using centrifugation.

Urine and fecal samples were collected for measurement of radioactivity, ruboxistaurin, N-desmethyl ruboxistaurin, and other potential metabolites. Urine was collected and samples pooled for 0-6 hour, 6-12 hour, 12-24 hour, 24 to 48 hour, 48 to 72 hour, and 72 to 96 hour intervals after dosing. Pooled urine collections continued for 24-hour intervals until radioactivity study release criteria, described below, were met. Each sample was weighed to determine volume, assuming a specific gravity of 1.0. Fecal samples were collected over 24-hour intervals until study release criteria were met. Samples were stored at  $-20^{\circ}\text{C}$  or  $-70^{\circ}\text{C}$  until analysis.

The release criteria stipulated that subjects were released from the study when excreted detectable radioactivity, normalized to a 24-hour interval, was equal to or less than 0.2% of the administered dose.

**Assay of Total Radioactivity:** All radioactivity calculations were based on the actual dose of 102  $\mu\text{Ci}$  and 66 mg of ruboxistaurin. Fecal samples were collected in polyethylene bags and homogenized on a Seward Manufacturing Lab Systems Model 3500 stomacher with a volume of tap water approximately equal to the fecal sample weight. If there were two or more samples within a 24 hour period, each sample was

DMD #9894

weighed and processed separately. The samples were processed either fresh or after thawing following storage at  $-20^{\circ}\text{C}$ . Three aliquots (approximately 0.3 to 1.0 g/aliquot) of each homogenate were oxidized using a Packard Model 307 Sample Oxidizer using Carbosorb® to absorb  $^{14}\text{C}$  and Permafluor E® as the liquid scintillant. Trapped  $^{14}\text{CO}_2$  was subsequently determined by liquid scintillation counting. Urine samples for the specified time periods were collected, weighed, kept on ice, and processed either fresh or after thawing following  $-20^{\circ}\text{C}$  storage. The radioactivity in 1 mL aliquots of urine was determined by liquid scintillation counting. Selected blood samples (approximately 0.2 g aliquots in duplicate or triplicate) were oxidized, and trapped  $^{14}\text{CO}_2$  was determined by liquid scintillation counting as for feces. The radioactivity in 1 mL aliquots of plasma was also determined directly by liquid scintillation counting techniques.

#### Radiolabeled Compound Quantification and Profiling in Plasma, Urine, and Feces:

Plasma: Plasma samples were frozen and stored at  $-20^{\circ}\text{C}$ . After thawing, each plasma sample (3 mL) was divided in half, processed in duplicate, and combined. For every 1.5mL plasma, 2 mL of acetonitrile were added and the mixture vortexed for approximately 30 seconds. The resulting sample was centrifuged at 3,000 RPM for 5 minutes. The supernatant was removed to a clean, labeled tube and the remaining plasma solids were vortexed with an additional 2 mL acetonitrile, centrifuged and supernatant removed. The remaining plasma solids were again vortexed with 2 mL acetonitrile, centrifuged and supernatant removed for a 3<sup>rd</sup> time. The supernatants were all combined and evaporated to dryness under nitrogen using a TurboVac at  $37^{\circ}\text{C}$ . The sample was reconstituted with 75  $\mu\text{L}$  acetonitrile + 175  $\mu\text{L}$  10 mM ammonium acetate. Recovery of radioactivity after extraction from the profiled plasma samples (from 4 hours to 24 hours)



DMD #9894

was  $89 \pm 18\%$  (mean  $\pm$  standard deviation (SD), N=7), and the total percent of each metabolite in plasma was adjusted accordingly. Radioactivity in plasma was profiled by HPLC with 96-well fraction collection, using a Waters 2690 Alliance module system with a Foxy 200 fraction collector and Deepwell LumaPlate-96 solid scintillator-coated plates. The plasma samples were applied to a YMC Basic (5  $\mu$ m particle size, 4.6 x 150 mm) column at ambient temperature and with a mobile phase flow rate of 1.0 mL/minute. The mobile phase solvents were 10 mM ammonium acetate buffer (A) and ACN (B) with the following gradient profile: (min/%B): 0/10, 50/60, 50.1/80, 52/80. The column effluent was collected into Deepwell Luma-96 solid scintillation-coated plates (Perkin Elmer Life and Analytical Sciences.) The recovery off the HPLC column was 115%. The Lumaplates were dried under centrifugal vacuum and counted on a Packard Microplate Scintillation & Luminescence counter (TopCount NXT). The CPM counts were plotted against time using ProFSA Plus version 3.1 software to obtain radioprofiles. The percent of each metabolite in plasma was calculated from the percent area of the radioactive peak of interest versus the total area of radioactivity above background in the sample radiochromatogram.

Urine: For each sample, 2 mL of urine were mixed with 5 mL of 0.4% formic acid solution. Water Oasis HLB (60 mg/3cc) SPE columns were prepared by rinsing with 3 mL methanol and then 3 mL Mill-Q water. The urine mixture was then loaded onto the SPE columns and the radioactivity eluted with 1 mL methanol followed by 1 mL 0.2% (v/v) ammonium hydroxide in methanol. This 2 mL elution solution was evaporated to dryness under nitrogen using a TurboVac at 37°C. The urine concentrate was reconstituted with 33.3  $\mu$ L acetonitrile + 66.7  $\mu$ L 10 mM ammonium acetate for injection

DMD #9894

into the HPLC system. The radioactivity in urine was profiled using the same HPLC conditions, and percent of each metabolite in urine was calculated as described for plasma. The percent of each metabolite was then multiplied by the percent dose excreted in that sample to calculate the percent dose comprised by that metabolite. The recovery after extraction from profiled urine samples (from 6 hours to 24 hours) from the SPE column was  $113 \pm 14\%$  (mean  $\pm$  SD, N=3) and the recovery off the HPLC column was 102%.

Feces: After thawing, an aliquot of the fecal homogenate (0.3 to 0.5 gms) was removed and shaken with 1.5 mL of acetonitrile on a Mistral multi-mixer for approximately 45 mins. The fecal mixture was centrifuge at 3,000 RPM for 5 minutes on a Beckman GPKR centrifuge. The supernatant was removed to a clean labeled tube and the remaining solids were shaken with 1.0 mL 50:50 (v/v) acetonitrile:water for an additional 45 mins. This fecal mixture was centrifuged at 3,000 RPM for 5 minutes and the 2<sup>nd</sup> supernatant was removed and added to the corresponding 1<sup>st</sup> supernatant. The combined supernatants for each sample evaporated to dryness under nitrogen using a TurboVac at 37°C. Each sample was reconstituted with 100  $\mu$ L acetonitrile + 300  $\mu$ L 10 mM ammonium acetate for injection into the HPLC system. The radioactivity in feces was profiled using the same HPLC conditions, and percent of each metabolite in feces was calculated as described for urine. The percent of each metabolite was also adjusted for the extraction recovery. The recovery after extraction from profiled fecal samples (from 24 hours to 144 hours) was  $91 \pm 23\%$  (mean  $\pm$  SD, N=9) and recovery off the HPLC column was 104%.

DMD #9894

## **Metabolite Characterization**

Samples were prepared for analysis as described above. Additionally, to detect metabolites at low levels, some plasma and urine samples were concentrated further. Selected plasma samples and selected pooled plasma samples were further concentrated 3 fold, 12 fold, and 24 fold by limiting the reconstitution volume. Selected urine samples were concentrated 20x and 50x. Urine samples were concentrated 20x using the extraction method described for radioprofiling. For the 50x concentration, 5 mL of urine was mixed with 10 mM ammonium acetate buffer, passed through Bond Elut Certify (130 mg/10 cc) SPE columns, eluted with methanol followed by 0.2% ammonium hydroxide in methanol, evaporated to dryness under nitrogen, and reconstituted in 100  $\mu$ L of ACN/10 mM ammonium acetate buffer (1:3) for injection into the HPLC system. Feces required no further concentration. The HPLC system consisted of a Shimadzu VP series (Shimadzu Scientific Instruments Inc., Columbia, MD) including a SIL-10AXL autosampler and a Surveyor PDA detector. Chromatographic separations were carried out either on a Phenomenex Synergi Polar-RP column (3.0 x 150 mm, 4  $\mu$ m particle size) with a flow rate of 0.4 ml/min or Waters YMC Basic column (3.0 x 150 mm, 5  $\mu$ m particle size; Waters Corporation). The mobile phase consisted of 10 mM aqueous ammonium acetate (mobile phase A) and acetonitrile (mobile phase B), and the analytes were eluted using a gradient profile (min/%B): 0/10, 5/10, 50/75, 50.1/90, 52/90. Mass spectrometric analysis was conducted on a Finnigan TSQ Quantum mass spectrometer (Thermo Electron Corporation, San Jose, CA) equipped with an electrospray ion source.

## **Assay for quantification of ruboxistaurin and N-desmethyl ruboxistaurin in Plasma**

DMD #9894

Plasma concentrations of ruboxistaurin and N-desmethyl ruboxistaurin were determined using a validated turbo ion spray LC/MS/MS analytical method using a SCIEX API 3000 atmospheric pressure ionization triple quadrupole mass spectrometer equipped with TurboIonSpray™ interface (Applied Biosystems, Concord, Ontario L4K 4V8), Shimadzu HPLC pumps (LC-10AD vp, Shimadzu Co., Columbia, MD 21046) and a Perkin-Elmer autosampler (Perkin-Elmer Series 200, Perkin-Elmer Corp., Norwalk, CT 06859). The assay demonstrated a lower limit of quantitation (LLQ) of 0.5 ng/mL. The calibration curves were fit by a weighted ( $1/x^2$ ) quadratic equation from 0.5 to 150 ng/mL. The coefficients of determination ( $r^2$ ) of the calibration curves were 0.9952 for ruboxistaurin and 0.9973 for N-desmethyl ruboxistaurin. Validation samples for ruboxistaurin and N-desmethyl ruboxistaurin were prepared at concentrations of 0.5, 80, and 150 ng/mL (six replicates per concentration) to determine the precision and accuracy of the human plasma assay. Validation intra-assay and inter-assay RSD for the validation samples ranged from 0.87 to 17.46% for ruboxistaurin and from 1.26 to 12.93% for N-desmethyl ruboxistaurin. The validation intra-assay and inter-assay RE for the VAL samples ranged from -2.67% to 6.92% (97% to 107% accuracy) for ruboxistaurin and from -8.52 to 15.80% (91% to 116% accuracy) for N-desmethyl ruboxistaurin.

The analytes were extracted from plasma samples (0.2 mL) prepared using a Isolute CBA (100 mg) 96-well extraction procedure. The extraction block was prepared by washing with 400  $\mu$ L methanol. Plasma samples with [2H6] ruboxistaurin added as the internal standard (IS), were mixed with 500  $\mu$ L of 10 mM ammonium acetate then loaded onto the prepared extraction block. Using a Tomtec Quadra 96-well sample processor, the cartridge bed was washed with 1 mL of water then 400  $\mu$ L of methanol. The bed was

DMD #9894

dried by applying full vacuum for 15 seconds after which the analytes were eluted off with 1 mL of 1% v/v formic acid in methanol. Each elute was evaporated to dryness under nitrogen using a TurboVac at 45°C. Each dried extract was reconstituted in 100  $\mu$ L 75:25v/v methanol:10 mM ammonium formate, pH 3.6 before analysis on a Shimadzu HPLC system. Extracted samples were analyzed using a Genesis CN 2.1 x 50 mm (4  $\mu$ m) HPLC column (Cat# FK5965E, Jones Chromatography USA Inc., Lakewood, CO 80228) and turbo ion spray LC/MS/MS in the positive ion mode. The isocratic mobile phase consisted of 20% Mobile Phase A (0.1% v/v trifluoroacetic acid in 5 mM ammonium formate, pH 3.6) and 80% Mobile Phase B (0.1% trifluoroacetic acid in methanol) at a flow rate of 200  $\mu$ L/min. QC samples containing ruboxistaurin and N-desmethyl ruboxistaurin at 1.5, 80 and 125 ng/mL were run with the study samples. The QC samples RSD ranged from 1.81 to 2.75% for ruboxistaurin and 1.61 to 3.45 for N-desmethyl ruboxistaurin. The QC samples RE ranged from -1.09 to 0.86% for ruboxistaurin and -1.85 to 4.13% for N-desmethyl ruboxistaurin. Sample stability has been demonstrated up to 290 days at -20C° in heparinized human plasma. The method was validated from 0.5 ng/mL to 150 ng/mL for both ruboxistaurin and N-desmethyl ruboxistaurin. The samples were analyzed at Advion BioScience, Inc (Ithaca, NY) US.

### **Data analysis for Pharmacokinetic Parameters**

Pharmacokinetic parameters for radioactivity, ruboxistaurin, and N-desmethyl ruboxistaurin (LY338522) were calculated using standard noncompartmental analyses of the plasma concentration versus time data. Analyses were performed WinNonlin Professional version 3.1 (Pharsight, Cary, NC), using the linear-log method of

DMD #9894

WinNonlin Model 200. These analyses were performed independently for total radioactivity, ruboxistaurin, and N-desmethyl ruboxistaurin data. The maximum plasma concentration ( $C_{\max}$ ) and the corresponding time of  $C_{\max}$  ( $t_{\max}$ ) were identified from observed data. The slope of the terminal log-linear portion of the concentration-time curve was estimated using unweighted least squares linear regression and was used to calculate the apparent elimination rate constant ( $\lambda_z$ ) and the apparent terminal half-life ( $t_{1/2}$ ), using the predicted concentration at the last sampling time ( $C'_{\text{last}}$ ). Area under the curve (AUC) estimates beyond the last measurable concentration were calculated as  $C'_{\text{last}}$  divided by  $\lambda_z$ . WinNonlin also calculated mean residence time (MRT), apparent plasma clearance (CL/F), and apparent volume of distribution ( $V_z/F$  and  $V_{ss}/F$ ) when possible. Pharmacokinetic parameters were estimated based on a ruboxistaurin dose of 66 mg.

## Results

Ruboxistaurin was well tolerated in all six subjects, all of whom completed the study according to the protocol. All calculations were based upon the 66-mg (102  $\mu\text{Ci}$ ) that was actually dosed, but is referred to as 64 mg (100  $\mu\text{Ci}$ ) targeted dose.

### Mass Balance of Total Radioactivity

Mass balance determination included urine and feces through the sample collection period of 21 days. The majority of the [ $^{14}\text{C}$ ]ruboxistaurin dose was excreted in feces with only a small amount excreted in urine as shown in Figure 2 and Table 1. Total recovery of radioactivity from the 6 subjects in this study was approximately 87.0%, with

DMD #9894

approximately  $82.6\% \pm 1.1\%$  of the radiocarbon dose recovered in the feces and approximately  $4.1\% \pm 0.3\%$  of the radiocarbon dose recovered in the urine. Excretion of fecal radioactivity appeared to plateau after 6 days, while the urinary excretion of radioactivity reached a plateau earlier.

### **Pharmacokinetics**

Plasma concentration curves are shown in Figure 3 and the key median pharmacokinetic parameters for plasma concentrations of total radiocarbon, ruboxistaurin, N-desmethyl ruboxistaurin (LY338522), and for combined concentrations of ruboxistaurin and N-desmethyl ruboxistaurin are shown in Table 2. The mean estimate of  $AUC_{(0-\infty)}$  for combined ruboxistaurin and N-desmethyl ruboxistaurin is about half that for plasma total radiocarbon, suggesting that about half the plasma radioactivity consisted of these two analytes. Ruboxistaurin and N-desmethyl ruboxistaurin comprised comparable fractions of the total radiocarbon in plasma, with means of 23% and 28%, respectively. Individual contributions ranged from 16% to 36%. The mean combined AUCs of ruboxistaurin and N-desmethyl ruboxistaurin accounted for about 52% of the total radiocarbon, while combined AUCs of ruboxistaurin and N-desmethyl ruboxistaurin in individual subjects ranged from 39% to 64%.

Ruboxistaurin concentrations in all plasma samples collected after 24 hours postdose were below the quantitation limit for ruboxistaurin, while N-desmethyl ruboxistaurin concentrations were quantifiable up to approximately 120 hours post dose. Plasma concentrations of total radiocarbon were detectable through at least 72 hours in all subjects, and in 3 subjects were detectable up to the last sampling time of 216 hours.

DMD #9894

The mean terminal half-life of total radiocarbon in plasma was longer than that of ruboxistaurin or N-desmethyl ruboxistaurin individually. The half-life of  $^{14}\text{C}$  reflects the composite half-life of ruboxistaurin and all of its metabolites and therefore represents a complex mixture of compounds with potentially widely varying individual half-lives. As such, it should be interpreted cautiously. The longer mean half-life of  $^{14}\text{C}$  could reflect the presence of a metabolite with a longer half-life than that of N-desmethyl ruboxistaurin, or it could be attributable to variability. Given the historically high variability in ruboxistaurin and N-desmethyl ruboxistaurin pharmacokinetics and the very wide range of 11.3 to 106 hours in half-life estimates for  $^{14}\text{C}$  (Table 2), variability is a plausible explanation for the relatively small difference between half-lives of N-desmethyl ruboxistaurin and total radiocarbon.

### **Metabolite Profiles in Plasma, Feces, and Urine**

For plasma, the recovery of radioactivity from the extraction steps was found to be 89%, and recovery from the HPLC column was determined to be approximately 100%, demonstrating that no major loss of radioactivity occurred from the plasma during sample preparation or analysis. Using LC/MS and LC/MS/MS evaluation described in previous work (Barbuch et al. 2006), ruboxistaurin and four metabolites were detected in plasma (Table 3). The four metabolites were **1**, the N-desmethyl of ruboxistaurin (LY338522); **2**, N,N-didesmethyl of ruboxistaurin; **3**, produced by hydroxylation at the 7-position of indole ring A (see Figure 1); and **6**, the N-oxide of ruboxistaurin (Table 4). Ruboxistaurin itself accounted for the majority of the total radioactivity at 4 and 8 hours (Table 3, Figure 4). The most abundant metabolite in plasma is **1** (N-desmethyl



DMD #9894

ruboxistaurin), representing approximately 16% and 11% mean percentage of total radioactivity at 4 hours and 8 hours, respectively. Ruboxistaurin and N-desmethyl ruboxistaurin combined comprised 39% to 64% of the radiocarbon AUC in plasma, indicating that N-desmethyl ruboxistaurin is the major metabolite. The other observed metabolites (**3**, **2**, and **6**) were present at much lower amounts as indicated in the table. The structures of the plasma metabolites were determined using MS/MS and confirmed using either standards (**1** and **2**) or NMR data (**3** and **6**) (Barbuch et al. 2006). Lower overall concentrations at 8, 12, and 24 hours led to fewer distinct radioactive peaks for identification, and all compounds were below the quantification limit (BQL) for radioactivity by 12 and 24 hours. Approximately 68% of the mean percent of the total radioactivity was identified as parent or a metabolite at 4 hours, dropping to approximately 45% at 8 hours, consistent with the pharmacokinetic results. Ruboxistaurin and a total of 16 metabolites were detected in urine using LC/MS/MS (Table 4), with unchanged ruboxistaurin representing less than 1% of the radioactive dose in urine. The major urinary metabolite based on the radiochromatograms was **1** (N-desmethyl ruboxistaurin), representing approximately 1% of the radioactive dose. Additional metabolites observed in human urine included **3** (7-hydroxy ruboxistaurin), **5**, and **27** (ruboxistaurin + O<sub>2</sub>) each representing less than 1% of the radioactive dose and **2**, **14**, **6**, **18**, **10**, **12**, **15**, **8**, **17**, **28**, **11**, and **9** each representing less than 0.1% of the radioactive dose (Figure 5). Table 5 shows the urinary metabolites and the corresponding percent of the radioactive dose they comprise. Based on LC/MS/MS analysis, ruboxistaurin and 14 metabolites were detected in feces (Table 4). Unchanged ruboxistaurin represented approximately 1% of the radioactive

DMD #9894

dose in feces. The major fecal metabolite based on the radiochromatograms was **1** (N-desmethyl ruboxistaurin), which represented approximately 28% of the radioactive dose eliminated in the feces. Additional metabolites observed in feces included **5**, **28**, **3**, **17**, **14**, and **2**. These six metabolites represent approximately 9%, 4%, 4%, 3%, 3%, and 2% of the radioactive dose eliminated in the feces, respectively. The definitive structures of both **5** and **3** have been confirmed using MS/MS and NMR. Metabolites representing 1% or less of the dose were **10**, **12**, **16**, **15**, **8**, **11**, and **29**. These metabolites are primarily hydroxylated products of either ruboxistaurin or **1**, N-desmethyl ruboxistaurin (Figure 6). Table 5 shows the fecal metabolites and the corresponding percent of the radioactive dose they comprise. A detailed description, with an explanation of the MS product ion spectra and when available NMR data, for ruboxistaurin and its metabolites is found in earlier work describing [<sup>14</sup>C]ruboxistaurin metabolism in animals (Barbuch et al. 2006).

## Discussion:

Ruboxistaurin and N-desmethyl metabolite (LY338522 or **1**) are potent and specific inhibitors of PKC  $\beta$ . The concentrations of N-desmethyl ruboxistaurin and ruboxistaurin were comparable in subjects given ruboxistaurin. Renal elimination of ruboxistaurin as a percent of dose is very minor, with the majority of the compound's clearance from the body appearing to be biliary and via the feces, consistent with preclinical models (Burkey et al. 2002, Barbuch et al. 2006). Mean cumulative total recovery of the administered radioactivity was 87%, and metabolites definitively identified in feces comprised 56% of that administered dose, with a total of 14 metabolites and unchanged ruboxistaurin identified in the feces. The majority of the

DMD #9894

metabolites in feces are primarily hydroxylated products of either ruboxistaurin or **1**, N-desmethyl ruboxistaurin. In general, this pattern of multiple hydroxylated metabolites holds true of the urinary metabolites as well.

Ruboxistaurin itself comprised only 1.3% of the excreted dose, indicating that it was extensively metabolized in this study. The largest proportion of the dose was eliminated as the N-desmethyl metabolite **1** (29.2%). Other more minor metabolites included **5** (9.4%), a hydroxylated N-desmethyl metabolite, and **3** (4.2%), a hydroxylated ruboxistaurin metabolite. These moieties represent the primary metabolic biotransformations for ruboxistaurin, as all other metabolites comprised less than 4% of the overall dose. The proposed primary metabolic pathways for ruboxistaurin biotransformation are N-desmethylation (to form **1**) and to a much lesser extent hydroxylation (to form **5** and **3**), as shown in Figure 7.

The plasma results in this study indicate that ruboxistaurin is absorbed into the systemic circulation following oral administration. The pharmacokinetics observed in this study are similar to those seen in previous clinical evaluations of the drug (Demolle, D., et al. 1998, Demolle, D., et al. 1999), with variable exposures seen subject to subject. Consistent with previous studies, the primary metabolite is N-desmethyl ruboxistaurin (**1**), and together, ruboxistaurin and N-desmethyl ruboxistaurin comprise approximately half of the circulating radioactivity in the plasma. The remaining radioactivity is comprised of multiple metabolites at extremely low levels, comprising 3% or less of the mean total radioactivity when they could be measured (**3**, **2**, **6**) and representing demethylation or addition of oxygen to the molecule. Further, there were 16 metabolites detected in the urine, all of which presumably were circulating in the blood and were

DMD #9894

filtered by the kidneys. The majority of these metabolites are primarily hydroxylated products of either ruboxistaurin or **1**, N-desmethyl ruboxistaurin. Detection and identification of metabolites in the plasma was complicated by the low level of radioactivity circulating in the plasma of the subjects in this study. Taken together, these data indicate that ruboxistaurin is extensively metabolized to multiple circulating metabolites, with only ruboxistaurin and N-desmethyl ruboxistaurin contributing significantly to the total circulating ruboxistaurin-related material.

Metabolism of ruboxistaurin in humans as reported in this paper is consistent with the metabolism of ruboxistaurin in preclinical species as previously reported (Barbuch et al. 2006). The major metabolite of ruboxistaurin in humans and preclinical species is the N-desmethyl ruboxistaurin metabolite **1**. Other metabolites include **2** and numerous hydroxy ruboxistaurin and hydroxy N-desmethyl ruboxistaurin metabolites. The majority of the metabolites were confirmed as being identical to the metabolites identified in dogs, mice, and rats. Metabolite **27** was identified as a dioxygenated product of ruboxistaurin but the absolute structure of this metabolite could not be discerned from the MS product ion spectrum. This metabolite was seen in dog feces but not previously reported due to very low concentrations. Metabolite **28** gives the same MS/MS data as the animal metabolite **7**, and the two metabolites are either identical to each other or may be diastereomers of one another. Metabolite **29** is an alcohol that is derived from the same metabolic pathway (of oxidative deamination to an aldehyde) as the acid **20** seen in animal species. All three metabolites are minor in humans and animals, and do not substantially contribute to the overall metabolism of the compound. Thus all metabolites identified in human were also identified in preclinical animal species or were generated

DMD #9894

in the same pathway as was seen in an animal species, and all metabolites circulating in humans were found circulating in animal species.

In conclusion, ruboxistaurin is absorbed upon oral administration, and both ruboxistaurin and its metabolites are eliminated primarily in the feces secondary to metabolism and biliary elimination. The majority of the excretion in both urine and feces occurred within one week of dosing. Ruboxistaurin and N-desmethyl ruboxistaurin are the major moieties in plasma, feces, and urine, comprising 52% of the circulating metabolites. Multiple additional metabolites are present in all three matrixes, but at significantly lower concentrations. Because these metabolites exist at such low concentrations, it is doubtful that they are of pharmacologic significance.

### **Acknowledgements**

The authors would like to thank Dr. Palaniappan Kulanthaivel and Dr. William Ehlhardt for their thoughtful scientific review and discussions of the data.

DMD #9894

## References:

- Aiello LP et al. The Effect of the PKC- Inhibitor Ruboxistaurin on Moderate Visual Loss: The PKC-DRS2 Trial Baseline Characteristics and Preliminary Results. Presented at the American Academy of Ophthalmology Annual Meeting, Chicago, IL, October 14, 2005.
- Aiello, L. P., Bursell, S., Devries, T., Alatorre, C., King, G., Ways, K (1999) Protein Kinase C $\beta$ -selective Inhibitor LY333531 Ameliorates Abnormal Retinal Hemodynamics in Patients with Diabetes. *Diabetes*. **48** Supplement 1:A19
- Ayo, S.H., Radnik R., Garoni, J.A., Troyer D.A., Kreisberg J.I. (1991) High glucose increases diacylglycerol mass and activates protein kinase C in mesangial cell cultures. *Am J Physiology* **261**:F571-F577.
- Barbuch, R.J., Campanale, K. M., Hadden, C. E., Zmijewski, M., Yi, P., O'Bannon, D. D., Burkey, J. L., and Kulanthaivel, P. (2006) In Vivo Metabolism of [14C]Ruboxistaurin in Dogs, Mice, and Rats Following Oral Administration and the Structure Determination of Its Metabolites by LC/MS and NMR Spectroscopy. *Drug Metab Dispos*, **34**:213-224.
- Beckman, J. A., Goldfine, A. B., Gorden, M. B., Garrett, L. A., Creager, M. A. (2002) Inhibition of Protein Kinase C $\beta$  Prevents Impaired Endothelium-Dependent Vasodilation Caused by Hyperglycemia in Humans. *Circulation Research* **90**: 107-111.

DMD #9894

Burkey, J.L., Campanale, K.M., O'Bannon, D. D., Cramer, J.W., and Farid, N.A. (2002) Disposition of LY333531, a selective protein kinase C $\beta$  inhibitor, in the Fischer 344 rat and beagle dog. *Xenobiotica*, **32**:1045-1052.

Craven, P.A., Davidson C.M., DeRubertis, F.R. (1990) Increase in diacylglycerol mass in isolated glomeruli by glucose from de novo synthesis of glycerolipids. *Diabetes* **39**:667-674.

Craven, P.A., DeRubertis, F.R. (1989) Protein kinase C is activated in glomeruli from streptozotocin diabetic rats. Possible mediation by glucose. *J. Clin Invest* **83**:1667-1675.

Danis RP, Bingaman DP, Jirousek MR, Yang Y. (1998) Inhibition of intraocular neovascularization caused by retinal ischemia in pigs by PKC  $\beta$  inhibition with LY333531. *Inves. Ophthal. Vis. Sci.* **39**: 171-179.

Demolle, D., de Suray, J.M., Vandenhende, F., and Onkelinx, C. (1998) LY333531 Single Escalating Oral Dose Study in Healthy Volunteers. *Diabetologia* **41**: [Suppl 1]: A 1 – A 354.

Demolle D, De Suray JM, Onkelinx C. (1999) Pharmacokinetics and safety of multiple oral doses of LY333531, a PKC beta inhibitor, in healthy subjects [abstract]. In: American Society for Clinical Pharmacology and Therapeutics 100th annual meeting; 1999 March 18-20; San Antonio. St. Louis (MO): Mosby, Inc. Clin Pharmacol Ther **65**(2):189. Abstract PIII-50

DMD #9894

DeRubertis, F.R., Craven, P.A. (1994) Activation of protein kinase C in glomerular cells in diabetes. Mechanisms and potential links to the pathogenesis of diabetic glomerulopathy. *Diabetes* **43**:1-8.

[ICRP]. The International Commission on Radiological Protection. (1990) Recommendation of the International Commission on Radiological Protection. *ICRP Publication* **60**. Oxford: Pergamon Press. p 6–25.

[NCRP]. National Council on Radiation Protection and Measurements. (1987) Summary and conclusions in: Ionizing radiation exposure of the population of the United States. *NCRP Report No. 93*. 52-60.

Inoguchi, T., Battan, R., Handler, E., Sportsman J.R. Heath W., King G.L. (1992) Preferential elevation of protein kinase C isoform  $\beta 2$  and diacylglycerol levels in the aorta and heart of diabetic rats: differential reversibility to glycemic control by islet cell transplantation. *Proc Natl Acad Sci USA* **89**:11059-11063.

Ishii H, Jirousek MR, Koya D, Takagi C, Xia P, Clermont A, Bursell S-E, Kern TS, Ballas LM, Heath WF, Stramm LE, Feener EP, King GL. (1996) Amelioration of vascular dysfunctions in diabetic rats by an oral PKC  $\beta$  inhibitor. *Science* **272**:728-731.

Jirousek MR, Gillig JR, Gonzalez CM, Heath WF, McDonald JH III, Neel DA, Rito CJ, Singh U, Stramm LE, Melikian-Badalian A, Baersky M, Ballas LM, Hall SE, Winneroski LL, Faul MM (1996) (S)-13-[(dimethylamino)methyl]-10,11,14,15-tetrahydro-4,9:16,21-dimetheno-1H,13H-dibenzo[e,k]pyrrolo[3,4-H][1,4,13]-



DMD #9894

oxadiazacyclohexadecene-1,3(2H)-dione (LY333531) and related analogues: isozyme selective inhibitors of protein kinase C $\beta$ . *J Med Chem* **39**:2664-2671.

Kikkawa, R., Haneda M, Uzu, T., Koya, D., Sugimoto, T., Shigeta, Y. (1994)

Translocation of protein kinase C  $\alpha$  and  $\zeta$  in rat glomerular mesangial cells cultured under high glucose conditions. *Diabetologia* **37**:838-841.

Kowluru R, Jirousek M, Stramm L, Engerman R, Kern T. (1996) Diabetes-induced

disorders of retinal protein kinase C and Na,K-ATPase are inhibited by LY333531. *Diabetes* **45 (S2)**:16A.

Kowluru RA, Jirousek MR, Stramm LE, Farid NA, Engerman RL, Kern TS. (1998)

Abnormalities of retinal metabolism in diabetes or experimental galactosemia. V. Relationship between protein kinase C ATPases. Retinal protein kinase C in diabetes. *Diabetes* **47**:464-469.

The PKC-DRS Study Group (2005) The effect of ruboxistaurin on visual loss in patients

with moderately severe to very severe nonproliferative diabetic retinopathy: initial results of the Protein Kinase C beta Inhibitor Diabetic Retinopathy Study (PKC-DRS) multicenter randomized clinical trial. *Diabetes*. **54**:2188-97.

Shiba, T., Inoguchi, T., Sportsman J.R., Heath, W.F., Bursell, S., King, G.L. (1993)

Correlation of diacylglycerol level and protein kinase C activity in rat retina to retinal circulation. *Am J Physiol* **265**:E783-E793.

Tuttle KR, Bakris GL, Toto RD, McGill JB, Hu K, Anderson PW (2005) The effect of

ruboxistaurin on nephropathy in type 2 diabetes. *Diabetes Care*. **28**:2686-90.

DMD #9894

Williams, B., Schrier, R.W. (1992) Characterization of glucose-induced in situ protein kinase C activity in cultured vascular smooth muscle cells. *Diabetes* **41**:1464-1472.

Williams, B., Schrier R. W. (1993) Glucose-induced protein kinase C activity regulates arachidonic acid release and eicosanoid production by cultured glomerular mesangial cells. *J. Clin Invest* **92**:2889-2896.

DMD #9894

**Footnotes NA**

## **Legends for figures**

**Figure 1: Structure of Ruboxistaurin: • mark site of radiolabeled carbon**

**Figure 2: Cumulative elimination (mean  $\pm$  SD) of total radioactivity in feces and urine after a single oral 64-mg (100 $\mu$ Ci) dose of  $^{14}$ C-ruboxistaurin to healthy male subjects (N=6).**

**Figure 3. Individual plasma concentration-time profiles for total radiocarbon (as quantitated by scintillation counting of plasma samples) (top panel), ruboxistaurin (as quantitated by LC-MS) (middle panel), and N-desmethyl ruboxistaurin (as quantitated by LC-MS) (LY338522; bottom panel) following oral administration of 64 mg  $^{14}$ C-ruboxistaurin in 6 healthy males. Note different axis scales.**

**Figure 4: Representative radiochromatogram of 8-hour human plasma sample after a single oral 64-mg (100  $\mu$ Ci) dose of  $^{14}$ C-ruboxistaurin mesylate.**

**Figure 5: Representative radiochromatogram of 0-6 hour human urine sample after a single oral 64-mg (100  $\mu$ Ci) dose of  $^{14}$ C-ruboxistaurin mesylate.**

**Figure 6: Representative radiochromatogram of 0-24 hour human fecal sample after a single oral 64-mg (100  $\mu$ Ci) dose of  $^{14}$ C-ruboxistaurin mesylate.**

DMD #9894

**Figure 7: Proposed primary metabolic pathways for the biotransformation of <sup>14</sup>C-ruboxistaurin in humans after a single oral 64-mg (100- $\mu$ Ci) dose of <sup>14</sup>C-ruboxistaurin.**

DMD #9894

**Tables:**

**Table 1. Cumulative (Mean  $\pm$  SD) Percentage of the Dose Excreted in Feces and Urine after a Single Oral 64-mg (100  $\mu$ Ci) Dose of  $^{14}$ C-Ruboxistaurin to Healthy Male Subjects (N=6)**

Time(hours)	Cumulative Percent Dose Excreted		
	Feces $\pm$ SD	Urine $\pm$ SD	Combined Totals
0-6	NA	0.8 $\pm$ 0.3	0.80
6-12	NA	1.6 $\pm$ 0.3	1.60
12-24	16.6 $\pm$ 15.7	2.4 $\pm$ 0.4	19.0
24-48	44.5 $\pm$ 33.5	3.0 $\pm$ 0.5	47.5
48-72	58.0 $\pm$ 25.4	3.3 $\pm$ 0.5	61.3
72-96	65.2 $\pm$ 21.0	3.5 $\pm$ 0.6	68.7
96-120	68.4 $\pm$ 22.2	3.7 $\pm$ 0.6	72.1
120-144	79.1 $\pm$ 3.1	3.8 $\pm$ 0.7	82.9
144-168	79.7 $\pm$ 3.2	3.8 $\pm$ 0.7	83.6
168-192	80.8 $\pm$ 2.7	3.9 $\pm$ 0.7	84.7
192-216	81.2 $\pm$ 2.7	3.9 $\pm$ 0.7	85.1
216-240	81.4 $\pm$ 2.7	4.0 $\pm$ 0.7	85.4
240-264	81.5 $\pm$ 2.6	4.0 $\pm$ 0.7	85.5
264-288	81.9 $\pm$ 2.6	4.0 $\pm$ 0.7	85.9
288-312	82.1 $\pm$ 2.6	4.0 $\pm$ 0.8	86.1
312-336	82.2 $\pm$ 2.7	4.0 $\pm$ 0.8	86.2
336-360	82.2 $\pm$ 2.7	4.1 $\pm$ 0.8	86.3
360-384	82.4 $\pm$ 2.7	4.1 $\pm$ 0.8	86.4
384-408	82.4 $\pm$ 2.7	4.1 $\pm$ 0.8	86.5
408-432	82.5 $\pm$ 2.6	4.1 $\pm$ 0.8	86.6
432-456	82.6 $\pm$ 2.6	4.1 $\pm$ 0.8	86.7
456-480	82.6 $\pm$ 2.6	4.1 $\pm$ 0.8	86.7
480-504	82.6 $\pm$ 2.6	4.1 $\pm$ 0.8	86.7
Total	82.6 $\pm$ 2.6	4.1 $\pm$ 0.8	87.0 <sup>a</sup>

Abbreviations: NA = not applicable, feces was collected over 24-hour intervals, SD = standard deviation.

<sup>a</sup> This total includes 0.3% of the dose recovered from toilet paper.

DMD #9894

**Table 2      Geometric Mean (CV%) Noncompartmental Pharmacokinetic  
 Parameter Estimates of Total Radiocarbon, Ruboxistaurin, N-desmethyl  
 ruboxistaurin (LY338522), and Ruboxistaurin + LY338522 Following Oral  
 Administration of 64-mg <sup>14</sup>C-Ruboxistaurin**

Pharmacokinetic Parameter	Units	Total Radiocarbon	Ruboxistaurin	LY338522	Ruboxistaurin + LY338522
N		6	6	6	6
<b>C<sub>max</sub></b>	nM or	367 (23.8)	204 (28.7)	87.4 (21.9)	NC
	nM-eq				
<b>t<sub>max</sub><sup>a</sup></b>	h	3.00	3.00	3.50	NC
		(1.00-6.00)	(1.00-5.00)	(1.00-6.00)	
<b>AUC (0-t<sub>last</sub>)</b>	nM h or	5620 (26.9)	1400 (25.5)	1630 (30.7)	3070 (22.0)
	nM-eq h				
<b>AUC (0-∞)</b>	nM h or	6130 (30.0)	1410 (25.8)	1700 (30.4)	3160 (21.8)
	nM-eq h				
<b>% AUC (t<sub>last</sub>-∞)</b>	%	6.87 (98.3)	1.02 (26.2)	4.00 (17.2)	NC
<b>λ<sub>z</sub></b>	h <sup>-1</sup>	0.0132 (106)	0.196 (9.35)	0.0195 (22.4)	NC
<b>t<sub>1/2</sub></b>	h	52.6	3.54	35.6	NC
		(106)	(9.35)	(22.4)	
<b>CL/F</b>	L/h	23.0 (30.0)	99.8 (25.8)	NC	NC
<b>V<sub>z</sub>/F</b>	L	1740 (72.4)	510 (23.1)	NC	NC
<b>MRT</b>	h	NC	5.83 (14.9)	NC	NC
<b>V<sub>ss</sub>/F</b>	L	NC	581 (22.1)	NC	NC

<sup>a</sup> median (minimum – maximum)

NC: not calculated.

Downloaded from dmd.aspetjournals.org at ASPET Journals on April 17, 2024

DMD #9894

**Table 3 Mean (N=6) Percent Radioactivity of Ruboxistaurin and Metabolites in Human Plasma after a Single Oral Administration of 64 mg [<sup>14</sup>C] Ruboxistaurin**

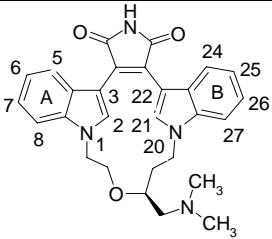
Plasma Sample ID: Metabolite	Mean Percent of Total Radioactivity per parent and metabolite	
	4hr	8hr
Ruboxistaurin	49.8	31.2
1	15.8	10.6
2	<1	BQL
3	<1	2.8
6	1.1	BQL

<sup>a</sup> Observed metabolite radioactivity as determined by 96 well fraction collection with scintillation counting and LC/MS/MS. Mean (n=6) total percent radioactivity per time point does not equal 100% since only distinct radioactive peaks were assigned values. Radioactivity peaks in 12- and 24-hour plasma samples were BQL (Below limit of quantification when < 8 cpms (2.3 ng) per radioactivity peak)



DMD #9894

**Table 4. Metabolites of <sup>14</sup>C-Ruboxistaurin in Human Plasma, Urine, and Feces after a Single Oral 64-mg (100 μCi) Dose of <sup>14</sup>C-Ruboxistaurin Mesylate to Healthy Male Subjects (N=6)**

Matrix <sup>a</sup>	Peak #	Metabolite ID <sup>b</sup>	M+H <sup>+</sup>	Product Ions, m/z
P U F	ruboxistaurin		469	451, 424, 406, 398, 384, 289, 98, 84, 58
P U F	<u>1</u>	N-desmethyl [LY338522]	455	424, 412, 406, 398, 384, 289, 84
P U F	<u>2</u>	N,N-didesmethyl [326986]	441	424, 423, 406, 398, 384, 289, 70
F	<u>29</u>	Alcohol [326651] N-dealkylation	442	424,399,384,371,353, 339, 313
U F	10 <sup>c</sup>	21-hydroxy-N-desmethyl	471	453, 440 428, 414, 197, 184, 156, 84
U F	17 <sup>d</sup>	A-ring hydroxy-N-desmethyl	471	454, 440, 428, 414, 289, 84
U	9 <sup>e</sup>	2-hydroxy-N-desmethyl	471	454, 428, 414, 271, 176, 169, 157, 145, 84
U F	5 <sup>d,f</sup>	7-hydroxy-N-desmethyl	471	453, 440, 428, 414, 396, 289, 84
U F	15 <sup>d</sup>	B-ring hydroxy-N-desmethyl	471	453, 440, 428, 414,305,84
U F	8 <sup>e</sup>	2-hydroxy-N-desmethyl	471	453, 440, 414, 271, 176, 169, 157, 145, 84, 70
U F	11 <sup>c</sup>	21-hydroxy-N-desmethyl	471	453, 440, 197, 184, 156, 84
U F	12	21-hydroxy	485	440, 422, 412, 400, 324, 184, 156, 98, 84, 58
U F	28 <sup>g</sup>	2-hydroxy [2053556]	485	440, 414,396, 384 271, 176, 169, 145, 84, 58
P U F	3 <sup>d,f</sup>	7-hydroxy	485	467, 440, 422, 414, 289, 98, 84, 58
U F	14 <sup>d</sup>	B-ring hydroxy	485	440, 305, 98, 84
F	16 <sup>d</sup>	A-ring hydroxy	485	440, 422, 414, 289, 84, 58
P U	6 <sup>d,f</sup>	N→O on dimethylamino	485	468, 467, 424, 289, 98, 84, 58
U	27	+ O <sub>2</sub>	501	483, 456, 438, 84, 58

Downloaded from dmd.aspetjournals.org at ASPET Journals on April 17, 2024

DMD #9894

U	18	+ O + glucuronide	661	485, 440
<p><sup>a</sup> P = plasma, U = urine, and F = feces</p> <p><sup>b</sup> The underlined metabolites in the table have been confirmed with either NMR or comparison with standards.</p> <p><sup>c</sup> Metabolites 10 and 11 product ion spectra suggest hydroxylation of the 21-position of indole ring B.</p> <p><sup>d</sup> Metabolites that have the m/z 289 product ion, have been hydroxylated on the indole ring A and conversely those with a m/z 305 ion have been hydroxylated on the indole ring B.</p> <p><sup>e</sup> The MS/MS product ion spectra for 8 and 9 are consistent with the two diastereomers of N-desmethyl 2053556. Metabolites 8 and 9 have the m/z 145, 169, 176, and 271 product ions consistent with hydroxylation of the 2-position of indole ring A in the keto form.</p> <p><sup>f</sup> Metabolite structures for 3, 5, and 6 have been determined with NMR (Barbuch et al. 2006).</p> <p><sup>g</sup> Metabolite 28 has been identified as LY2053556 based on its MS/MS product ion spectrum and its relative retention time compared with the standard. Metabolite 28 has m/z 145, 169, 176, and 271 ions, consistent with hydroxylation at the 2-position of indole ring A (Barbuch et al. 2006).</p> <p><sup>h</sup> Metabolite 18 has been identified as the glucuronide of hydroxylated parent but the MS/MS data was not sufficient to determine the site of hydroxylation.</p>				

DMD #9894

**Table 5. Mean (N=6) Percent of Dose Excreted in Urine and Feces Identified as Ruboxistaurin and Metabolites from Healthy Male Subjects After a Single Oral Administration of 64 mg <sup>14</sup>C-Ruboxistaurin**

Metabolite ID	%Dose represented by metabolite <sup>a</sup>		
	Urine (0 to 48 hr)	Feces <sup>b</sup> (0 to 120hr)	Total
ruboxistaurin	<1.0	1.2	1.3
1 (LY338522)	1.1	28.0	29.2
5	<1.0	9.2	9.4
3	<1.0	4.1	4.2
28 <sup>c</sup>	<1.0	3.9	3.9
17	<0.1	3.0	3.1
14	c	2.5	2.5
2 <sup>c</sup>	<0.1	1.8	1.8
10 + 12	<0.1	1.1	1.1
Total radioactivity identified <sup>d</sup>	2.3	57.2	59.5
Total radioactivity excreted	3.0	78.2	81.2

Downloaded from dmd.aspetjournals.org at ASPET Journals on April 17, 2024

DMD #9894

- a Metabolite percentages have been adjusted for the extraction recovery results of approximately 91% for feces and approximately 100% for urine.
- b For Subject 4027, 0 to 144 hr fecal samples were examined.
- c In urine, 2 elutes with 14, and 15 elutes with 28.
- d Metabolite 11, 8, 15, 27, 16, 29, 9, 18, and 6 each represented <1.0% of the total dose and are not included in the totals.

Abbreviations: 1 = N-desmethyl ruboxistaurin; 2 = N,N-didesmethyl ruboxistaurin; 17, 10, 5, 15, 8, 11, 9 = N-desmethyl ruboxistaurin + O; 3, 14, 12, 16, 28 = ruboxistaurin + O; 29 = dealkylated ruboxistaurin (alcohol); 6 = N-oxide of ruboxistaurin; 27 = ruboxistaurin + O<sub>2</sub>; 18 = ruboxistaurin + O + glucuronide.

---

Figure 1

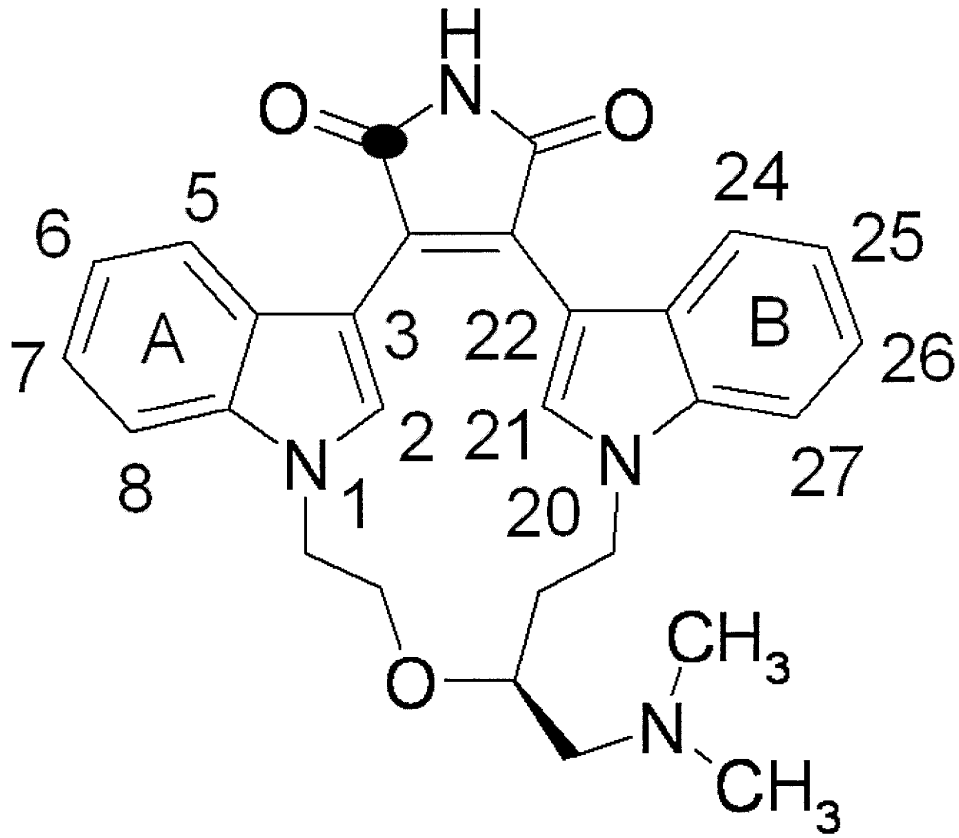
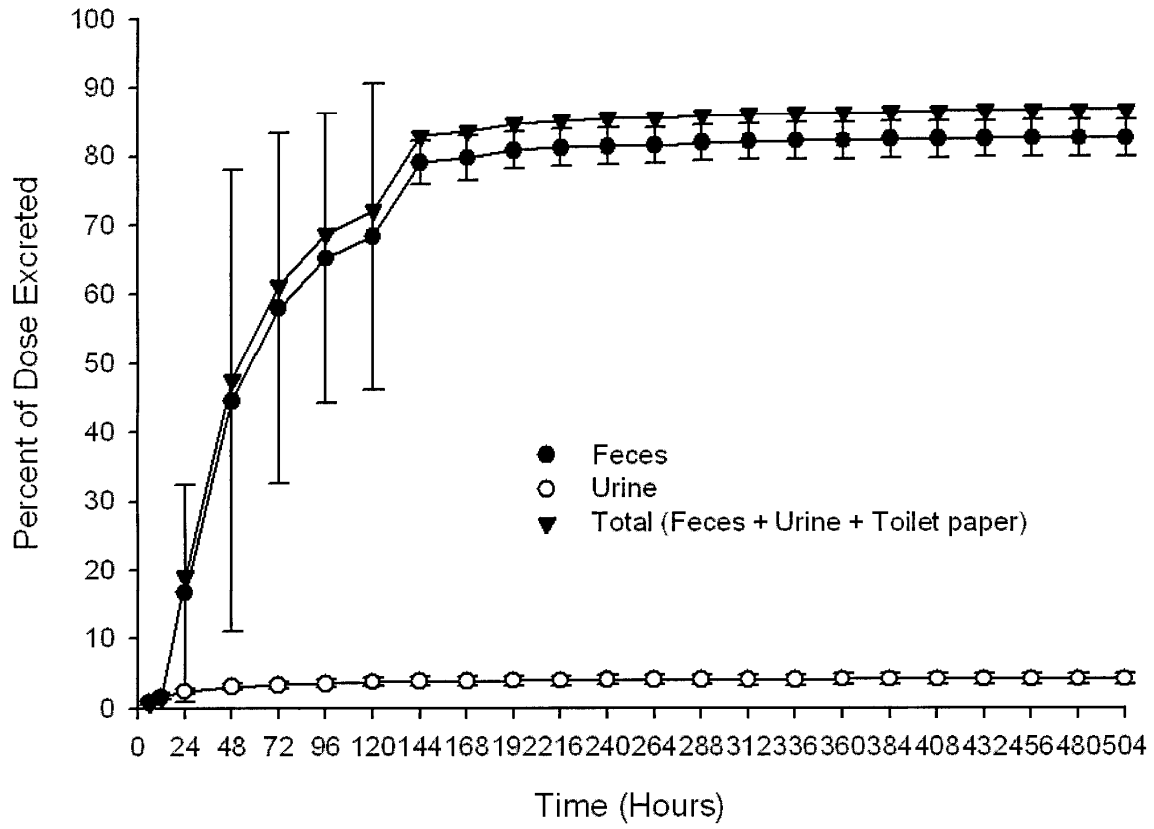


Figure 2



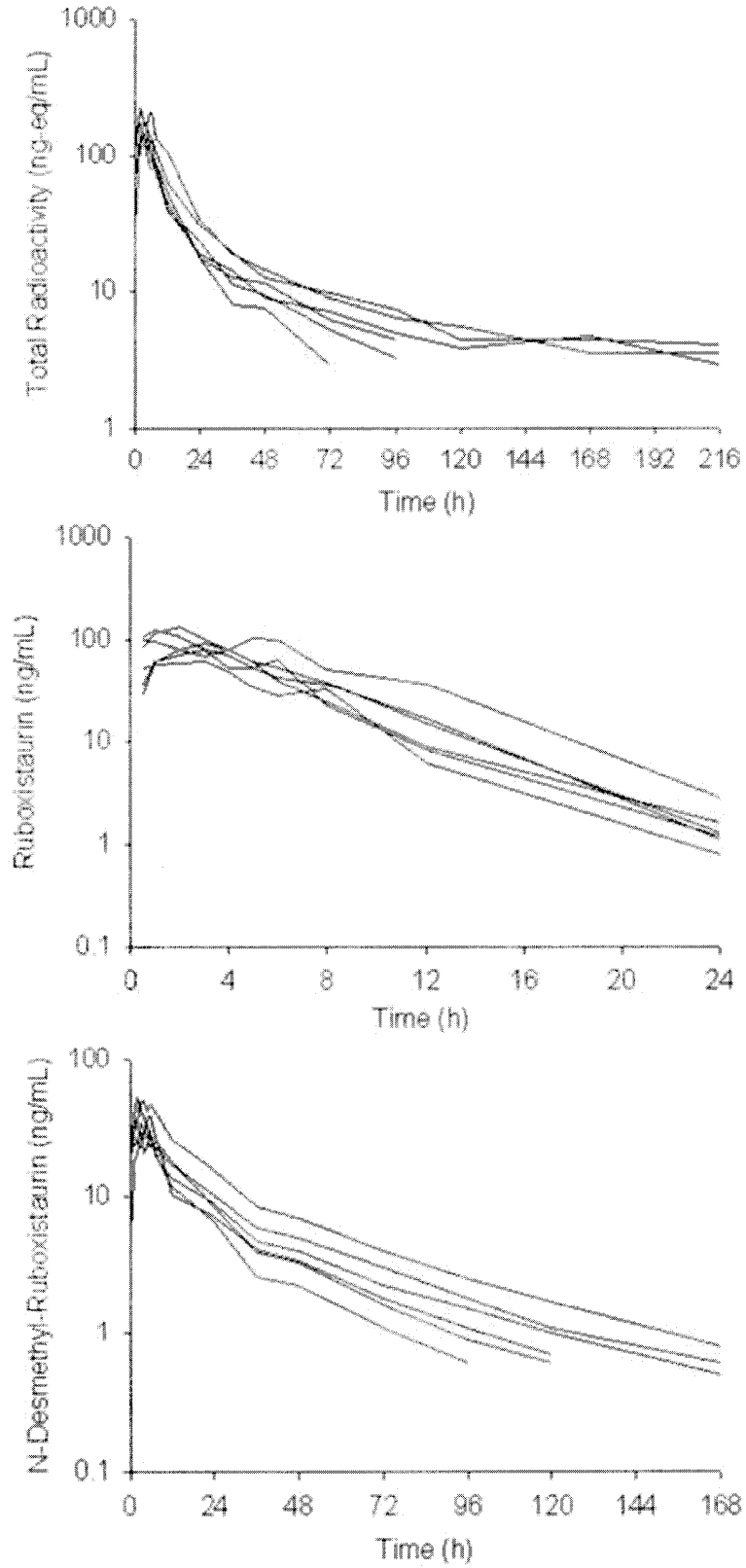


Figure 3

Figure 4

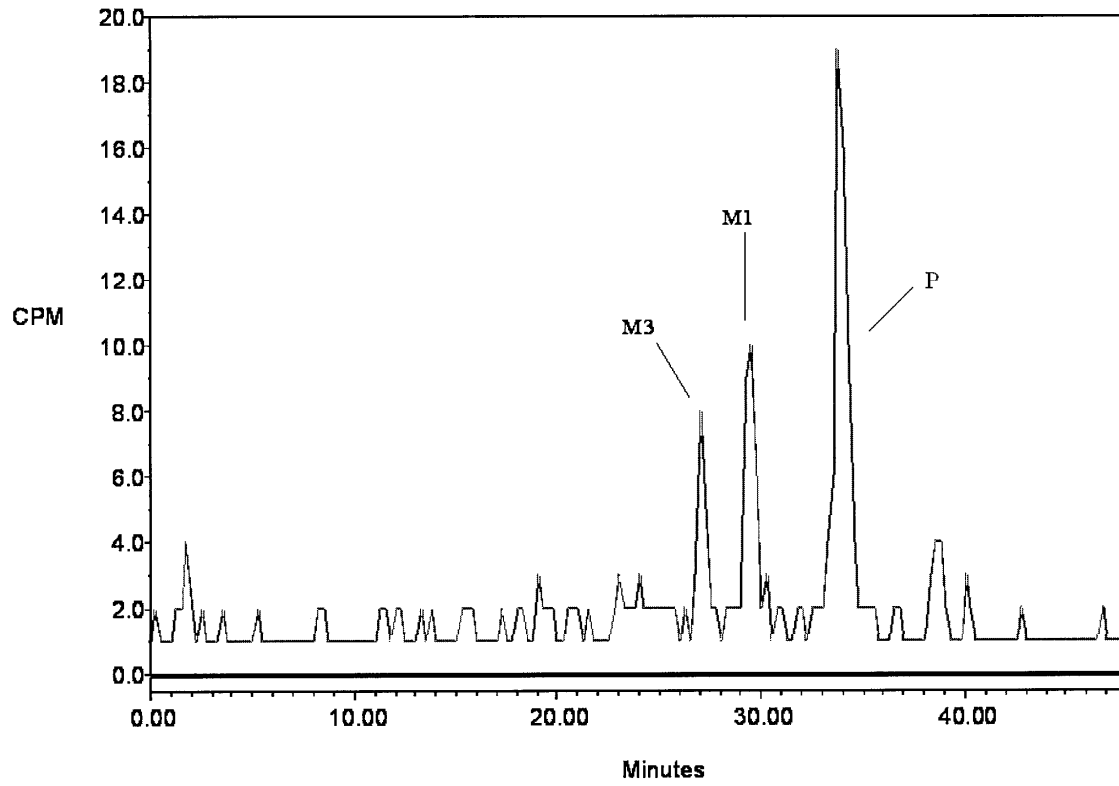




Figure 5

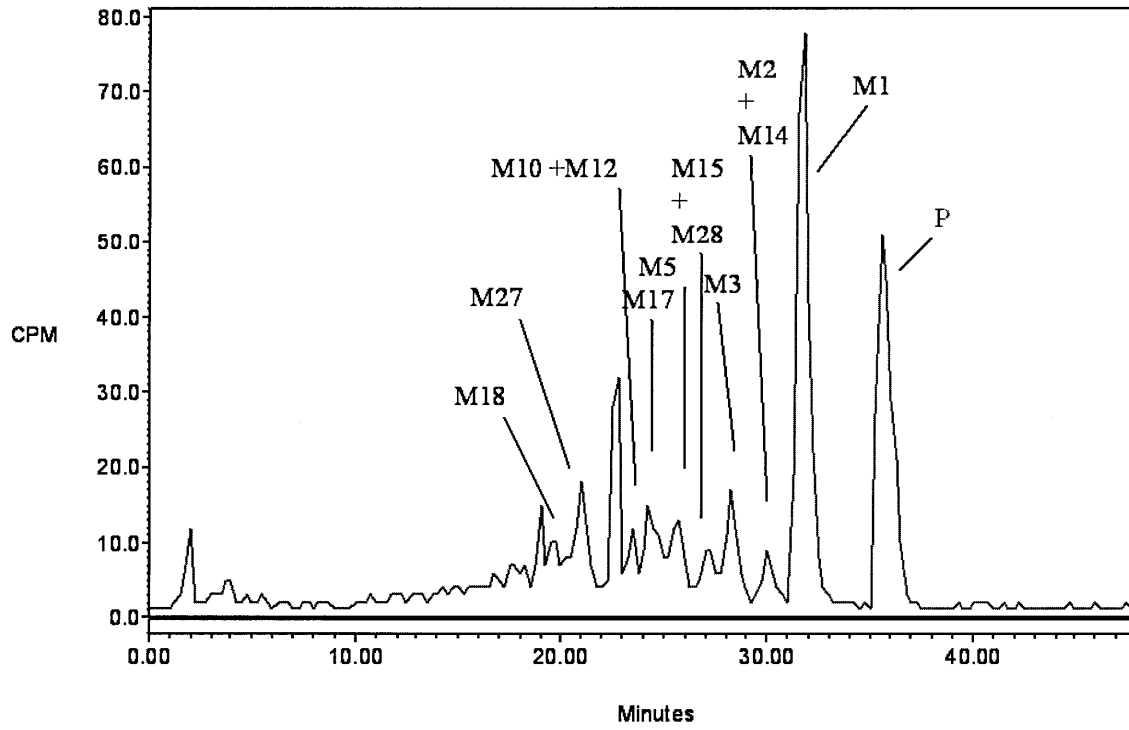
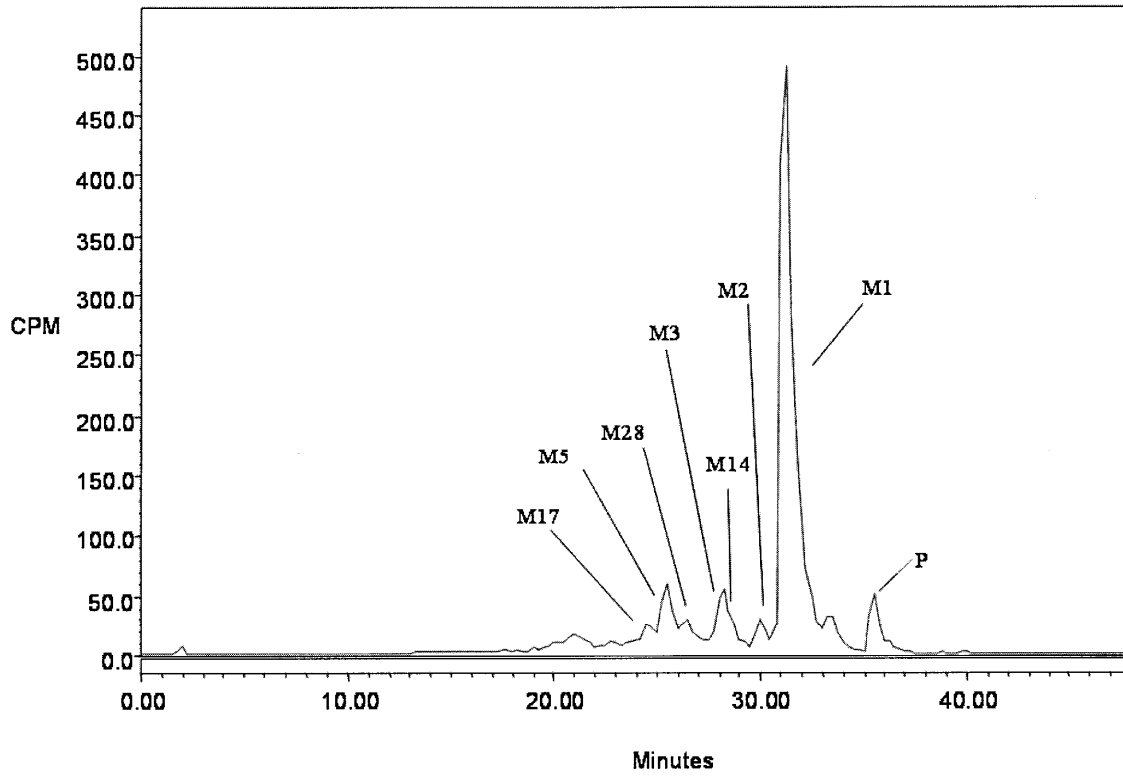


Figure 6



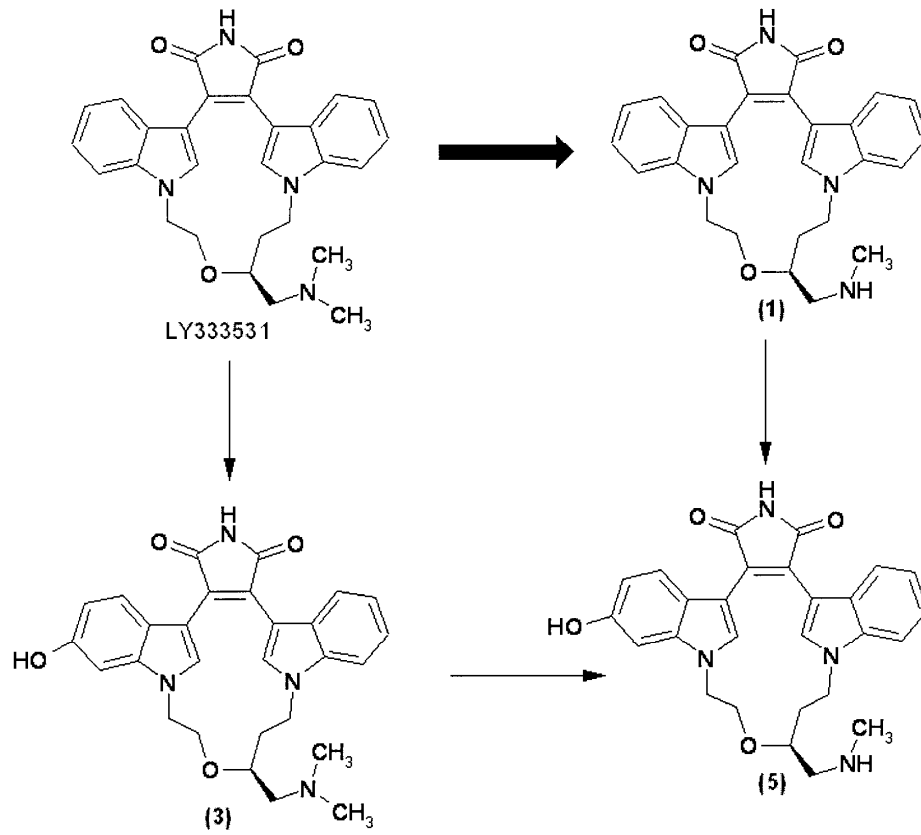


Figure 7